Extension of Generalized Hammerstein Model to Non-Polynomial Inputs

Antonin Novak, Laurent Simon and Pierrick Lotton
Laboratoire d'Acoustique de l'Université du Maine, UMR CNRS 6613
Le Mans, FRANCE
Email: http://ant-novak.com/

***Abstract*—The Generalized Hammerstein model has been successfully used during last few years in many physical applications to describe the behavior of a nonlinear system under test. The main advantage of such a nonlinear model is its capability to model efficiently nonlinear systems while keeping the computational cost low. On the other hand, this model can not predict complicated nonlinear behaviors such as hysteretic one. In this paper, we propose an extension of the Generalized Hammerstein model to a model with non polynomial nonlinear inputs that allows modeling more complicated nonlinear systems. A simulation provided in this paper shows a good agreement between the model and the hysteretic nonlinear system under test.**

I. Introduction

Many real-world systems exhibit nonlinear characteristics that must be taken into account when modeling such systems [1]. Consequently, identifying a nonlinear system (NLS) is an important challenge in many areas of experimental science.

During last few decades many nonlinear models have been studied in order to fit the nonlinear behavior of physical systems. Some of them are based on a knowledge of the physical system under test whereas others perform without any physical assumption. The latter, so-called black-box model, is often used since a very little knowledge about the nonlinear phenomena of the physical system under test is known.

Among these black-box models, the Generalized Hammerstein model has drawn a particular attention in the field of audio, acoustics, and mechanical vibrations. It has been used successfully in modeling nonlinear systems such as an audio limiter [2], an electrodynamic loudspeaker [3] a piano soundboard [4] or an acoustic waveguide [5]. However, although the Generalized Hammerstein model is capable of modeling nonlinear systems with a nonlinear law being frequency dependent, they fail in modeling nonlinear systems where the effects of input to the system are experienced with a high delay in time, such as systems with hysteresis.

In this paper, we propose an extension of the traditional Generalized Hammerstein model that would be able to deal with more complicated nonlinearities such as hysteresis. The Generalized Hammerstein model is first introduced in section II. The theoretical background for the proposed extension and the identification procedure are then discussed in section III. In section IV, we successfully study a simulated hysteretic system using the proposed method. Finally, we provide a discussion and a conclusion in sections V and VI.

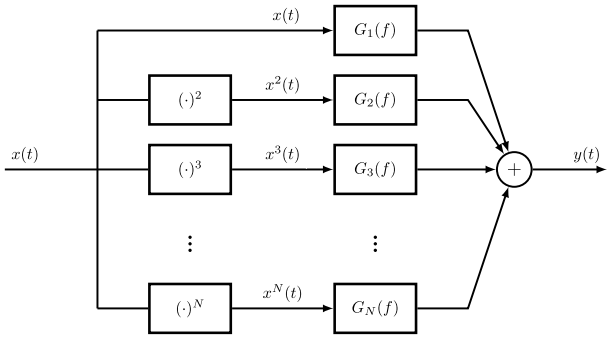

Fig. 1. Traditional Generalized Hammerstein model with polynomial functions.

II. Generalized Hammerstein Model

The identification of a nonlinear system using a Generalized Hammerstein model (Fig.1) consists in estimating the unknown linear filters $G_n(f)$ from the known input and output signals $x(t)$ and $y(t)$ respectively. The Generalized Hammerstein model consists of parallel branches, each branch represented by static nonlinearity and a linear filter $G_n(f)$. The static nonlinearity of a given branch n is usually a polynomial with output $x^n(t)$ as depicted in Fig. 1. The filters $G_n(f)$ are usually estimated from so-called Higher Harmonic Frequency Responses (HHFRs) using a matrix transform between both [2], [6].

We recall that, given an input signal $x(t)$ and an output signal $y(t)$ of a NLS, the HHFR $\mathcal{H}_l^{(y,x)}(f)$ may be seen as the contribution, in both amplitude and phase, of the l-th harmonic at the output, for a sine at frequency f at the input, as

$$\mathcal{H}_l^{(y,x)}(f) = |\mathcal{H}_l^{(y,x)}(f)|e^{j\varphi_l^{(y,x)}(f)}. \tag{1}$$

In [7], Chebyshev polynomials are used as nonlinear inputs instead of classical polynomial inputs. Such a modification lead to filters $G_n(f)$ that are directly equal to HHFRs and, therefore, no matrix transform needed.

In the following we show, that the nonlinear functions in each branch of the Generalized Hammerstein model can be of any desired form and we provide a transform relation between the corresponding linear filters of each branch of the model and the HHFRs.

978-0-9928-6265-7/16/$31.00 ©2016 IEEE

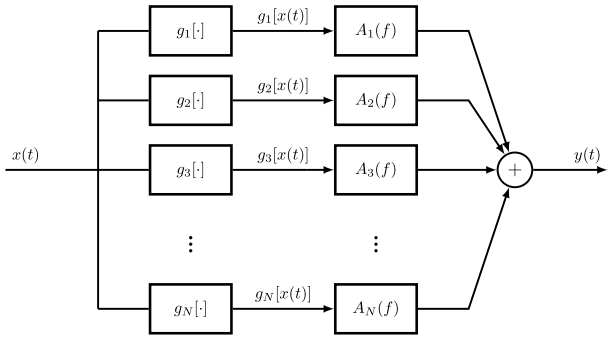

Fig. 2. Proposed extended Generalized Hammerstein model with nonlinear functions $g_n[x(t)]$ and linear filters $A_n(f)$, $n \in [1, N]$.

III. Extension of Generalized Hammerstein Model to Non-Polynomial Inputs

A. Model definition

The traditional Generalized Hammerstein model can be extended from polynomial-based model to a model based on a set of nonlinear functions of our choice. In such a case, the model is made up of N parallel branches, each branch consisting of a linear and/or a nonlinear function $g_n[x(t)]$ followed by a linear filter $A_n(f)$ (Fig. 2). As shown later in this paper, the nonlinear functions $g_n[x(t)]$ used in this work can be chosen as any linear and/or nonlinear functions with memory process including functions with a hysteretic behavior.

The output signal $y(t)$ of the nonlinear system can then be expressed in frequency domain as

$$Y(f) = \sum_{n=1}^{N} \text{FT}\{g_n[x(t)]\} A_n(f), \tag{2}$$

where $Y(f) = \text{FT}\{y(t)\}$, FT representing the Fourier Transform.

Note that extending the Generalized Hammerstein model to arbitrary nonlinear functions $g_n[x(t)]$ give more degrees of freedom than a traditional polynomial based Generalized Hammerstein model. Thus, the identification procedure consists first in the choice of the set of nonlinear functions $g_n[x(t)]$ and second in the estimation of the linear filters $A_n(f)$.

B. Identification process

In order to estimate the linear filters $A_n(f)$ we need first measure the HHFRs. Several methods have been developed to estimate the HHFRs. The most intuitive, but time-consuming one is based on a harmonic excitation of the system under test and the process is repeated by changing the input frequency step by step. In [8], two methods have been proposed, the first one being based on FFT techniques to estimate the auto-spectrum and phase information of HHFRs and the second one using IQ demodulation. In this paper, the so-called Synchronized Swept-Sine Method [6] is used to estimate the HHFRs, but any other technique allowing the estimation of $\mathcal{H}_l^{(y,x)}(f)$ in both amplitude and phase can be used.

The Synchronized Swept-Sine is generated using [6]

$$x(t) = \sin\left[2\pi f_1 L \exp\left(\frac{t}{L}\right)\right]. \tag{3}$$

where

$$L = \frac{T}{\ln\left(\frac{f_2}{f_1}\right)}, \tag{4}$$

and where f_1 and f_2 are initial and final frequency respectively and T is duration of the swept-sine. Note, that the definition of the exponential swept-sine (Eq. (3)) does not contain the "-1" term contrary to the usual definition [9]. For more details about why the term "-1" should not appear in the exponential swept-sine definition please refer to [6].

The HHFRs are then calculated using a deconvolution of the measured signal $y(t)$ with a so-called inverse filter as

$$h(t) = \mathcal{F}^{-1}\left[\mathcal{F}[y(t)]\tilde{X}(f)\right], \tag{5}$$

where the Fourier transform of inverse filter $\tilde{X}(f)$ is given analytically as

$$\tilde{X}(f) = 2\sqrt{\frac{f}{L}} \exp\left\{-j2\pi f L\left[1 - \ln\left(\frac{f}{f_1}\right)\right] + j\frac{\pi}{4}\right\}. \tag{6}$$

The impulse response $h(t)$ then consist of time-delayed higher harmonic impulse responses, separated by time delays $\Delta t_n = L\ln(n)$, that can be windowed and represented in the frequency domain as the $\mathcal{H}_l^{(y,x)}(f)$. For more details see [6].

Another important step in the identification procedure is the choice of the nonlinear functions $g_n[x(t)]$. They can be chosen as polynomials, that is equal to the traditional Generalized Hammerstein model [2], or the Chebychev-polynomial based model [7] or they can be chosen thanks to a partial knowledge of the physical system under test. We can, e.g., keep few polynomial branches and add one branch with a hysteretic law to include this nonlinear phenomenon to the model.

The identification consists next in the resolution of a linear system of N equations using the least squares method. First, the coefficients $c_{n,k}$ of Discrete Fourier Series of the functions $g_n[x(t)]$ are calculated as

$$c_{n,k} = \frac{2}{M}\sum_{m=0}^{M-1} g_n\left[\sin(\frac{2\pi}{M}m)\right] \exp\left(-j\frac{2\pi}{M}km\right), \tag{7}$$

for an input signal being a discrete-time harmonic signal of length M. Next, the following set of linear equations with unknown $A_n(f)$ is solved

$$H_i(f) = \sum_{n=1}^{N} A_n(f) c_{n,i} + \text{Res}(f), \tag{8}$$

for $i \in (1, I)$ and $n \in (1, N)$, $\text{Res}(f)$ being the residue. As $I \geq N$, there can be more equations than unknowns. To solve the set of equations (8) for $I > N$, the least squares algorithm [10] is then applied, minimizing the residue $\text{Res}(f)$.

If the functions $g_n[x(t)]$ are improperly chosen, the value of the residue increases drastically. This makes the residue $\text{Res}(f)$ an *a posteriori* criterion for the correct or improper choice of nonlinear functions $g_n[x(t)]$.

TABLE I
ESTIMATED VALUES OF THE PARAMETERS α, β AND γ (TEN TIMES AVERAGING BY TIME SYNCHRONOUS AVERAGING).

SNR	15	20	25	30	35	40	∞
mean(α)	1.05	1.01	1	1	1	1	1
mean(β)	0.21	0.2	0.2	0.2	0.2	0.2	0.2
mean(γ)	0.55	0.52	0.5	0.5	0.5	0.5	0.5
mean($Res(f)$)	$4.1 \cdot 10^{-4}$	$1.4 \cdot 10^{-4}$	$4.5 \cdot 10^{-5}$	$1.4 \cdot 10^{-5}$	$4.5 \cdot 10^{-6}$	$1.4 \cdot 10^{-6}$	$6 \cdot 10^{-13}$

IV. SIMULATION EXPERIMENT

In this section, the identification procedure described in previous sections is tested on simulated data. We focus on the identification of an NLS exhibiting quadratic hysteresis effects. Such type of hysteresis is dominant, e.g., in propagating waves in inhomogeneous media [11].

The simulated system under test used in the following is chosen from the field of nonlinear acoustic propagation in materials with hysteretic nonlinearity [12]. The chosen input-output law represents the relation between stress and strain. It is defined as

$$y(t) = \alpha x(t) + \beta x^2(t) + \gamma q[x(t), x_m], \tag{9}$$

where the linear part $\alpha x(t)$ and the nonlinear non-hysteretic part $\beta x^2(t)$ are combined with a quadratic hysteresis $q[x(t), x_m]$ defined as [12]

$$q[x(t), x_m] = x_m x(t) - \frac{1}{2}\left(x_m^2 - x^2(t)\right) sign\left(\frac{\partial x(t)}{\partial t}\right), \tag{10}$$

$sign$ being the signum function and x_m the past extreme value of the input excitation signal $x(t)$. The hysteresis loop of the quadratic hysteresis $q[x(t), x_m]$ consequently depends on input excitation parameter x_m, as shown in Fig. 3. The equation (9) may be seen as a semi-empirical input-output law for which the hysteresis model fits well the experimental data.

The identification consists then in the estimation of parameters α, β and γ. We first test the method on a static hysteretic system with no frequency dependency. In this experiment, a white Gaussian noise (WGN) is furthermore added to evaluate the robustness of the method in the presence of output noise. Next, a dynamic hysteresis nonlinearity with frequency dependent coefficients $\tilde{\alpha}(f)$, $\tilde{\beta}(f)$ and $\tilde{\gamma}(f)$ is simulated.

The method proposed in this paper allows, first, to separate the linear, the nonlinear and the hysteretic parts, secondly, to analyze the frequency dependency of the weights (or model parameters) of each part and, lastly, to estimate the global nonlinear model.

The sampling frequency is $f_s = 96kHz$ and the frequency range $[f_1, f_2]$ of the excitation signal is [300 Hz, 3.5 kHz].

A. Static Hysteresis Nonlinearity

In the first example, we consider a static hysteretic nonlinearity with frequency independent coefficients α, β and γ. For the simulation, they are set to arbitrary values $\alpha = 1$, $\beta = 0.2$ and $\gamma = 0.5$. As the system under test is not frequency dependent, the filters $A_1(f)$, $A_2(f)$ and $A_3(f)$ have constant values that are equal to α, β and γ. A WGN $n(t)$ is added to the output signal (Fig. 4) to evaluate the robustness of the method.

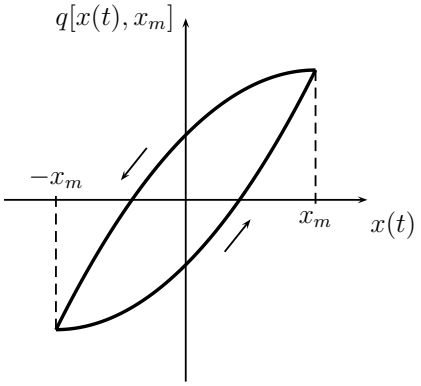

Fig. 3. The hysteresis loop of the quadratic hysteresis $q[x(t), x_m]$, x_m being the past extremum value of the input signal.

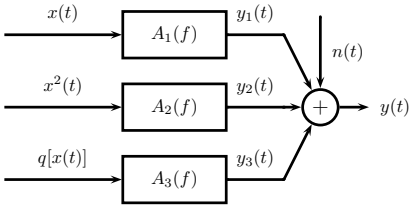

Fig. 4. The nonlinear hysteretic system with a WGN $n(t)$ added to the output.

Table I gives both the estimated mean values of parameters α, β and γ for different output signal-to-noise ratios (SNR), and the corresponding mean values of the residue $Res(f)$. The mean value of all the measured parameters is calculated within the frequency range $[f_1, f_2]$. The estimated values of the parameters are in good agreement with the available simulated data, leading to errors less than 10% for SNR=15 dB (worst simulated case). Similarly, the mean value of the residue is about 500 times below the weakest parameter value to be estimated, for SNR=15 dB. Lastly, the error between the estimated mean values and the exact values may be reduced by time synchronous averaging of output signals.

B. Hysteresis Nonlinearity with Frequency Dependency

In the second simulated case, a dynamic hysteretic system is considered. The input-output model defined in Eq. (9) is

TABLE II
MEAN SQUARED ERROR (MSE) OF THE ESTIMATED PARAMETERS.

	$A_1(f)$	$A_2(f)$	$A_3(f)$
amplitude MSE [dB]	-104	-119	-105
phase MSE [rad]	$4 \cdot 10^{-4}$	$8 \cdot 10^{-5}$	$7 \cdot 10^{-4}$

simulated with frequency-dependent coefficients $\tilde{\alpha}(f)$, $\tilde{\beta}(f)$ and $\tilde{\gamma}(f)$. From the NLS identification point of view, the frequency-dependent coefficients are equivalent to the Frequency Response Function (FRF) of each branch. For this simulation, the FRF $\tilde{\alpha}(f)$, related to the linear part of the NL system, is chosen as a one degree-of-freedom (1-DOF) system, presenting a resonant frequency $f_\alpha = 1kHz$. The FRF $\tilde{\beta}(f)$, related to the non-hysteretic quadratic part of the NL system, is also chosen as a 1-DOF system, presenting a resonant frequency $f_\beta = 2kHz$. Lastly, the FRF $\tilde{\gamma}(f)$, related to the quadratic hysteresis, is chosen as a 2-DOF system, with resonant frequencies $f_{\gamma_1} = 1kHz$ and $f_{\gamma_2} = 2.6kHz$.

The Figs. 5-7 show both simulated FRFs $\tilde{\alpha}(f)$, $\tilde{\beta}(f)$ and $\tilde{\gamma}(f)$, and estimated FRFs $A_1(f)$, $A_2(f)$ and $A_3(f)$ (amplitude and phase), and the associated magnitude error and phase error. The value of the output SNR is 30 dB. For the sake of clarity, the estimated FRFs are depicted as dashed lines 10dB below their values in modulus and 0.8 radian below in phase. Whatever the considered FRF, the agreement between simulated and estimated values is very good, both in modulus and phase, for all the bandwidth of analysis. This is also confirmed by the values of associated magnitude error and phase error. The magnitude error of the FRFs is indeed at least 20dB below the lowest value of the modulus of the FRFs. For the phase error, the maximum of the error is less than 1% of the phase values in the passband, and increases in the stopbands and near the antiresonance areas of $\tilde{\gamma}(f)$. Lastly, the mean-square errors (MSE) associated to the estimations of $A_1(f)$, $A_2(f)$ and $A_3(f)$ are given in Table II. The results prove that the method can successfully estimate the frequency-dependent coefficients with a minimal model error.

V. DISCUSSION

It has been shown in a simulated system that the proposed extension of the Generalized Hammerstein model can take into account more complicated sources of nonlinearities such as hysteresis. However, it is important to note that the knowledge of a possible hysteretic law must be known a priori. This is a case of many physical systems [12], [11] in which the proposed method would be beneficial. On the other hand, if the nonlinear system under test is completely unknown, the nonlinear functions $g_n[x(t)]$ can be chosen as polynomial functions. This choice approaches the traditional Generalized Hammerstein model. Several different set of functions $g_n[x(t)]$ can be tested; the residue $\text{Res}(f)$ may serve as a criterion to best choice of $g_n[x(t)]$.

Another example of using the extended Generalized Hammerstein model might be a purely asymmetric nonlinearity. In such a case, the only odd powers of the polynomials $x^n(t)$ can be kept decreasing the computing power consumption of the model.

In addition, inverse polynomials can be considered as nonlinear functions $g_n[x(t)]$ as a possible choice for models used in nonlinear inverse problems.

VI. CONCLUSION

In this paper, an extension of the Generalized Hammerstein model using non-polynomial nonlinear functions is proposed and tested in a simulation of a hysteretic nonlinear system. It has been shown that the method can estimate the frequency dependency of systems parameters in amplitude and phase very precisely. Two numerical experiments have been set up for estimating the coefficients of a given hysteretic law: a simulation for which the coefficients are frequency independent, and a simulation for which the coefficients are frequency dependent. In the first case, the robustness of the method has been successfully tested by adding output noise for different SNR, and by estimating the coefficients of the NLS. In the second case, it has been shown that the method estimates accurately the frequency-dependent coefficients of the NLS.

REFERENCES

[1] G. Bertotti and I. Mayergoyz, *The Science of Hysteresis*. Academic Press, 2006.

[2] A. Novak, L. Simon, F. Kadlec, and P. Lotton, "Nonlinear system identification using exponential swept-sine signal," *Instrumentation and Measurement, IEEE Transactions on*, vol. 59, no. 8, pp. 2220–2229, 2010.

[3] M. Rébillat, R. Hennequin, É. Corteel, and B. F. Katz, "Identification of cascade of hammerstein models for the description of nonlinearities in vibrating devices," *Journal of Sound and Vibration*, vol. 330, no. 5, pp. 1018–1038, 2011.

[4] K. Ege, X. Boutillon, and M. Rébillat, "Vibroacoustics of the piano soundboard:(non) linearity and modal properties in the low-and mid-frequency ranges," *Journal of Sound and Vibration*, vol. 332, no. 5, pp. 1288–1305, 2013.

[5] A. Novak, B. Maillou, P. Lotton, and L. Simon, "Nonparametric identification of nonlinear systems in series," *Instrumentation and Measurement, IEEE Transactions on*, vol. 63, no. 8, pp. 2044–2051, 2014.

[6] A. Novak, P. Lotton, and L. Simon, "Synchronized swept-sine: Theory, application, and implementation," *Journal of the Audio Engineering Society*, vol. 63, no. 10, pp. 786–798, 2015.

[7] A. Novak, L. Simon, P. Lotton, and J. Gilbert, "Chebyshev model and synchronized swept sine method in nonlinear audio effect modeling," in *Proc. 13th Int. Conference on Digital Audio Effects (DAFx-10)*, 2010.

[8] P. Nuij, O. Bosgra, and M. Steinbuch, "Higher-order sinusoidal input describing functions for the analysis of non-linear systems with harmonic responses," *Mechanical Systems and Signal Processing*, vol. 20, no. 8, pp. 1883–1904, Nov. 2006.

[9] A. Farina, A. Bellini, and E. Armelloni, "Non-linear convolution: A new approach for the auralization of distorting systems," in *AES 110th convention*, Amsterdam, May 2001.

[10] G. Strang, *Introduction to Applied Mathematics*. Wellesley, Massachusets: Wellesley-Cambridge, 1986.

[11] V. Gusev and V. Tournat, "Amplitude-and frequency-dependent nonlinearities in the presence of thermally-induced transitions in the preisach model of acoustic hysteresis," *Physical review B. Condensed matter and materials physics*, vol. 72, no. 5, pp. 54 104–54 104, 2005.

[12] V. Gusev, "Propagation of acoustic pulses in material with hysteretic nonlinearity," *The Journal of the Acoustical Society of America*, vol. 107, p. 3047, 2000.

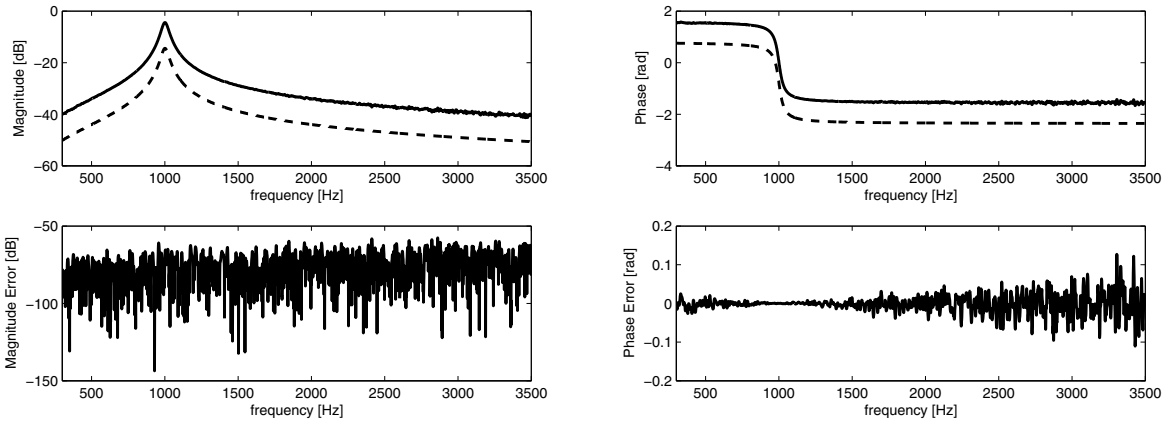

(a) (b)

Fig. 5. Amplitude (a) and phase (b) of the theoretical filter $\tilde{\alpha}(f)$ (solid) and estimated filter $A_1(f)$ (dashed and shifted of -10dB offset in amplitude and -0.8 rad in phase) and its difference (below) for AWGN of SNR = 30dB.

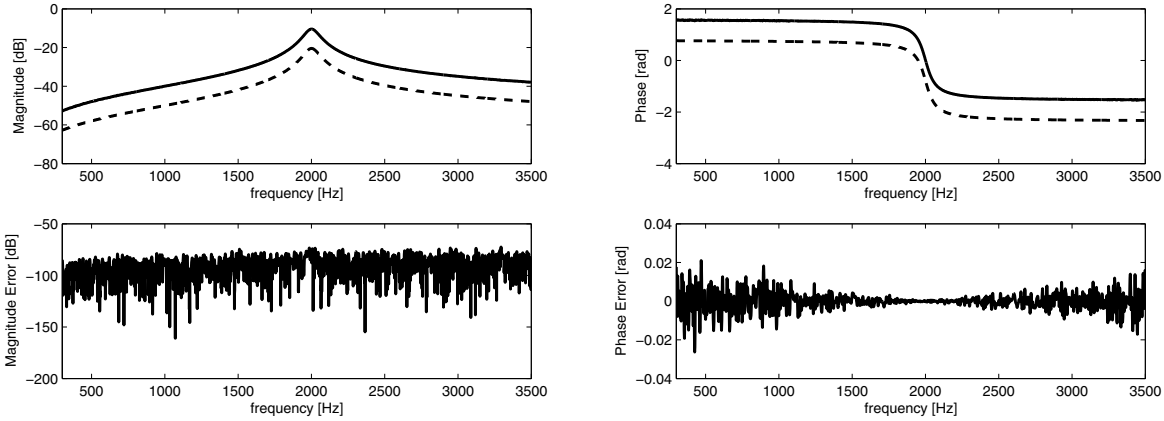

(a) (b)

Fig. 6. Amplitude (a) and phase (b) of the theoretical filter $\tilde{\beta}(f)$ (solid) and estimated filter $A_2(f)$ (dashed and shifted of -10dB offset in amplitude and -0.8 rad in phase) and its difference (below) for AWGN of SNR = 30dB.

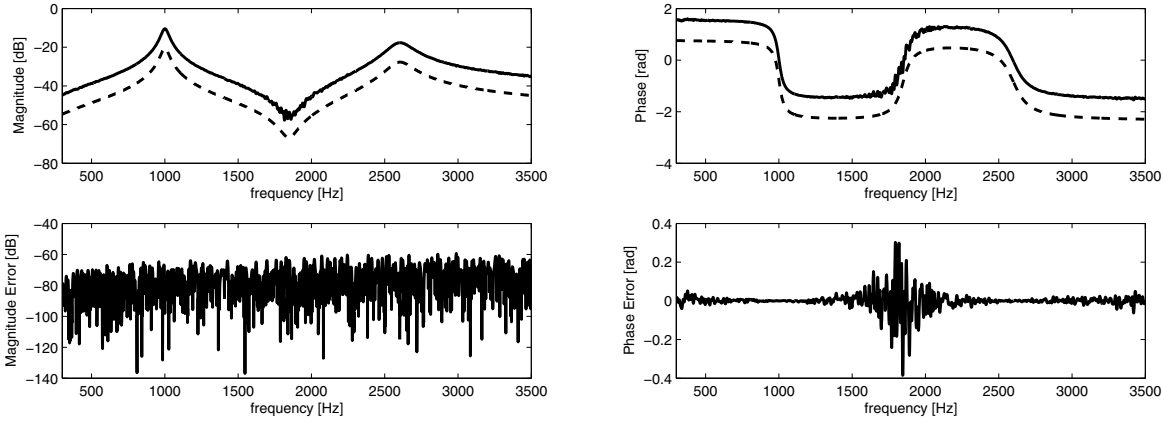

(a) (b)

Fig. 7. Amplitude (a) and phase (b) of the theoretical filter $\tilde{\gamma}(f)$ (solid) and estimated filter $A_3(f)$ (dashed and shifted of -10dB offset in amplitude and -0.8 rad in phase) and its difference (below) for AWGN of SNR = 30dB.